

Modern Raman Microscopy

Modern Raman Microscopy:

Technique and Practice

By

Alexander Rzhevskii

**Cambridge
Scholars
Publishing**



Modern Raman Microscopy: Technique and Practice

By Alexander Rzhevskii

This book first published 2021

Cambridge Scholars Publishing

Lady Stephenson Library, Newcastle upon Tyne, NE6 2PA, UK

British Library Cataloguing in Publication Data

A catalogue record for this book is available from the British Library

Copyright © 2021 by Alexander Rzhevskii

All rights for this book reserved. No part of this book may be reproduced, stored in a retrieval system, or transmitted, in any form or by any means, electronic, mechanical, photocopying, recording or otherwise, without the prior permission of the copyright owner.

ISBN (10): 1-5275-6784-2

ISBN (13): 978-1-5275-6784-9

Dedicated to Mechislav and Bronislav Rzhevskii

TABLE OF CONTENTS

Preface	x
Acknowledgements	xiv
Chapter One.....	1
Fundamentals of the Raman Effect and Raman Spectroscopy	
1.1. The sky is blue and the sunset is red due to light being scattered.....	2
1.1.1. Fundamentals of Raman scattering.....	7
1.2. Fundamentals of Raman spectroscopy	20
1.2.1. Selection rules in vibrational spectra.....	20
1.2.2. Ellipsoid of polarizability	24
1.2.3. Normal modes of molecular vibrations	28
1.2.4. Frequencies and transitions in vibrational spectra.....	32
1.2.5. Intensities in vibrational spectra.....	37
1.2.6. Principles of molecular symmetry.....	47
1.2.7. Characteristic (group) frequencies.....	56
1.3. Excitation wavelengths and fluorescence	59
1.4. Polarization	69
1.5. Advantages of Raman spectroscopy	79
Chapter Two	88
Raman Microscopy Instrumentation	
2.1. Evolution of Raman Instrumentation	88
2.2. Lasers	95
2.2.1. Types of lasers.....	96
2.2.2. Wavelength options.....	108
2.2.3. Beam quality	112
2.2.4. Power and brightness.....	116
2.2.5. Spectral linewidth.....	119
2.2.6. Frequency and power stability.....	123
2.3. Microscope.....	125
2.3.1. Microscope objectives	127
2.3.2. Sampling stages.....	137
2.3.3. Beamsplitters	139
2.3.4. Blocking Rayleigh scattered light.....	142

2.4. Spectrograph	149
2.4.1. Diffraction gratings	151
2.4.2. Detectors	163
2.4.3. Types of spectrograph configurations	183
2.4.4. Resolving power of a spectrograph	188
2.4.5. Optical throughput of a spectrograph	199
2.5. Microscope-to-spectrometer coupling optics	203
2.6. Optical components maintenance and cleaning	208
2.7. Some key aspects to consider when choosing a Raman microscope	212
Chapter Three	219
Confocal Raman Microscopy and Imaging	
3.1. Basic principles of confocal Raman microscopy	219
3.1.1. The role of confocal aperture (pinhole)	220
3.1.2. Optical alignment and calibration	226
3.1.3. Raman maps and images	232
3.1.4. Focused laser beam and sampling volume element.....	235
3.2. Mechanisms and conditions of sample mapping.....	246
3.3. Evaluation of spatial resolution and sensitivity of confocal Raman microscopes.....	261
3.4. Confocal Raman measurement of samples with irregular surfaces.....	271
3.5. Raman measurements beyond the diffraction limit of light	275
3.6. Designers and producers of Raman microscopes.....	280
3.6.1. Bruker.....	281
3.6.2. CRAIC Technologies	283
3.6.3. Edinburgh Instruments	284
3.6.4. Horiba Scientific	285
3.6.5. JASCO.....	287
3.6.6. Nanophoton	289
3.6.7. Renishaw	291
3.6.8. SOL Instruments	294
3.6.9. Thermo Fisher Scientific	296
3.6.10. WITec.....	299
3.7. Some practical aspects of working with confocal Raman imaging microscopes.....	302

Chapter Four	311
Selected Examples of Raman Microscopy and Imaging Applications	
4.1. Polymer composites and laminated polymer films	312
4.2. Pharmaceutical dosage forms and formulations.....	321
4.3. Biological cells, bacteria and tissues.....	328
4.4. Nanomaterials	343
4.5. Raman and photoluminescence imaging in mineralogy and gemology	354
4.6. The accurate measurement of spectral shifts in the Raman spectrum of Silicon.....	361
4.7. Fluorescence and Raman imaging for the detection of gunshot residue for forensic purposes.....	365
Appendix	376
Single Vibration and Group Frequencies Commonly Observed in Raman Spectra	

PREFACE

In 1928, Sir C.V. Raman discovered the phenomenon of inelastic light scattering. The radiation scattered by molecules contains photons of the same frequency as the incident radiation, as well as photons with frequencies shifted with respect to that of the incident radiation. The frequency change was named the Raman effect after Sir Raman, and the phenomenon of scattering these photons is called Raman scattering. In 1928, Sir C.V. Raman was awarded the Nobel Prize for his discovery. The Raman effect formed the basis of a new method of vibrational spectroscopy and, by the end of the 1930s, Raman spectroscopy has become the experimental method for nondestructive chemical analysis.

IR spectroscopy surpassed Raman spectroscopy after World War II, when the development of sensitive IR detectors and advances in electronics made IR spectroscopy easier to use. Measurements using IR spectroscopy became routine, while Raman spectroscopy still required sophisticated equipment, skilled operators and a dark room.

With the development of lasers in the 1960s, interest in Raman spectroscopy rose again, but its application was mostly limited to research laboratories. Skilled operators were still required to collect simple spectra, and the process was rather labor intensive.

The subsequent progress in Raman instrumentation, such as the introduction of sensitive charge-coupled devices for detection of inelastically scattered light and holographic filters for the rejection of elastically scattered

(Rayleigh) radiation, marked the beginning of the renaissance of Raman spectroscopy as a routine laboratory technique.

Confocal optical microscopy, which was pioneered by Marvin Minsky in 1955, and the coupling of a Raman spectrometer with a conventional optical microscope, commercially realized as the Molecular Optical Laser Examiner (MOLE) in 1976, opened up a new era in confocal Raman microscopy. It provided nondestructive analysis of the interior of optically transparent and translucent objects, as well as novel materials and systems at the microscopic level.

Modern confocal Raman scanning microscopy, which allows one to acquire two-dimensional and three-dimensional spectrochemical images of samples, is a unique method not only due to the information obtained but also in terms of the technologies involved in this technique. Indeed, the experimental implementation of this technology combines methods of spectroscopy, optics, electronics, mechanics and microscopy. The power and diversity of this technology also allow it to be used for a wide range of applications: from cell biology, forensic science and analysis of works of art to material science and the study of substances in various states, as well as under external impacts in real time.

Today, confocal Raman microscopes are computer-driven instruments equipped with multiple laser excitation sources, precise sample scanning mechanisms, white light and Raman polarization capabilities, automatic alignment and calibration procedures. These advantages make the measurements of Raman spectra and the acquisition of spectrochemical images with a spatial resolution at the diffraction limit of light a routine procedure. Advanced algorithms for the processing of spectral data arrays

and the availability of a wide range of Raman spectral libraries facilitate the representation and interpretation of the results.

The purpose of this book is to familiarize a wide circle of experimenters with the fundamentals of the technique and practice of confocal Raman microscopy and imaging. The author has tried to present the theory of Raman spectroscopy, instrumentation, principles of operation and the main characteristics of confocal Raman microscopes in a thorough but accessible form. Examples of the application of Raman microscopy and imaging for some of the most frequently used applications are provided.

The first chapter of this book is devoted to the basics of vibrational spectroscopy. Although the main vibrational spectroscopy techniques, such as Raman and modern FTIR spectroscopies, are complementary, it is necessary to understand their benefits for the optimal choice of the spectral method when studying specific chemical compounds and samples.

The second chapter describes the main components of Raman microscopes and the basic principles of their operations. The importance of choosing the most optimal components and the proper configuration of Raman microscopes is emphasized in order to obtain the best possible experimental results for specific applications.

The third chapter provides the specifics of Raman microscopes' confocal design. It highlights the importance of maintaining these instruments in a technical condition that ensures their maximum performance and capabilities. A separate part of this chapter is devoted to the different manufacturers of commercial confocal Raman microscopes, listing the models of the instruments produced, their main characteristics and capabilities.

In the final, fourth chapter, some examples of applications of confocal Raman microscopy and imaging are given, which illustrate the possibilities of this technique for obtaining two- and three-dimensional spectrochemical images of “real world” objects in order to study their spatial structure, composition and properties.

This book is intended for a wide circle of experimenters from a diversity of disciplines, who are using or intending to use confocal Raman spectroscopy and imaging methods in their work. Since this book was written for experimenters with different backgrounds, the author did not provide an exhaustive bibliography on the topics discussed. References are given, as a rule, only to the results of research over the past 10–15 years where the problem was presented most fully (mainly reviews) and to some classical primary sources. The author hopes that this book will be beneficial for novice Raman microscopy users and serve as a reference resource for experienced spectroscopists.

ACKNOWLEDGEMENTS

I am grateful to Dr. Ellen Misseo for her kind assistance in writing this book and for her valuable remarks and corrections. I would also like to thank Vadim Pushkarchuk and Pavel Ermakovich for their inestimable help in creating illustrations for this book.

CHAPTER ONE

FUNDAMENTALS OF THE RAMAN EFFECT AND RAMAN SPECTROSCOPY

1.1. The sky is blue and the sunset is red due to light being scattered

The interaction of light, a form of electromagnetic radiation, with matter results in the reflection, absorption, transmission and scattering of light. In some cases, this interaction also results in photoluminescence, that is, the light emissions at longer wavelengths than that of the incident light. It is generally accepted that the phenomenon known as the molecular scattering of light was first considered and explained in the works of Lord Rayleigh, who, among other aspects of scattering theory, calculated the degree of light scattered by molecules of atmospheric dust-free gases. John William Strutt, the future famous physicist Lord Rayleigh, was challenged by James Clerk Maxwell to explain the blue colour of the sky; he addressed this issue from the viewpoint of the wave theory of light. According to Rayleigh, a light wave propagating in the atmosphere causes oscillations in air molecules followed by the emission of light waves. Each molecule is independent of other emitters of secondary waves, and to calculate the intensity of the scattered light, it is enough to sum up the secondary radiation of individual molecules. He found that the amount of the scattered light I was inversely proportional to the fourth power of wavelength λ of the light for the particles that were much smaller than the wavelength:

$$I \propto 1/\lambda^4. \quad (1.1)$$

We will be referring to this dependence, which was established by Rayleigh in 1871, through the text of this book, as it plays an important role in the spectroscopy of scattered light. Since the portion of the electromagnetic spectrum visible to the human eye occupies the wavelength range from about 400 (violet) to 800 (dark red) nanometers (nm), then, for example, the blue light of 450 nm is scattered more intensely than the red light of 670 nm by a factor of $(670/450)^4 \approx 5$. Thus, Rayleigh first successfully explained the blue colour of the sky—the blue colour has a shorter wavelength than the red and yellow, so the blue rays of the sunlight are scattered stronger. When we look overhead to the sky on a clear cloudless day, not directly to the sun, the sky appears to be blue because we observe the light scattered by the molecules in the atmosphere, and scattered light is mostly blue. When we look in the direction of the sun at the sunset or sunrise, we see red and orange colours because the light from the sun passes a long distance through the atmosphere and the blue light scatters out and away from the line of observation.

The scattering of light by molecules, which Rayleigh studied to explain the blue colour of the sky, occurs without changing the frequency of the light—the frequency of the scattered light is equal to the frequency of the incident. Such scattering is called elastic since the state of the molecule after scattering is the same as before. This is the dominant scattering of light by particles much smaller than the wavelength of the radiation, and this process is called Rayleigh scattering. The scattering occurs in all directions uniformly and can be extended to scattering from the particles up to about a tenth of the wavelength of light. Another type of elastic scattering, Mie

scattering, occurs from spherical particles with dimensions comparable to or slightly larger than the wavelength of the incident light. In this process, the scattered radiation does not depend much on the wavelength. This effect gives rise to the scattered white light seen in clouds, mist or fog, and the bright whiteness of snow.

In 1923, the Austrian physicist Adolf Smekal published a theoretical paper in which he gave a clear prediction of the phenomenon of inelastic scattering of photons of light by atoms and molecules (Smekal 1923). Smekal suggested that, as the result of scattering, shorter and longer wavelengths would appear in addition to the original wavelength of light. Smekal also assigned the frequency shift between the incident and scattered light to the energy difference between the two states of the molecule: before and after scattering. The Dutch, Hans Kramers, and the German, Werner Heisenberg, strengthened the prediction of Smekal in a more expanded form (Kramers and Heisenberg 1925), which was later followed by the quantum-mechanical descriptions proposed by English theoretical physicist Paul Dirac (Dirac and Fowler 1927).

According to quantum theory, atoms and molecules can only take on certain discrete values of energy E_0 , E_1 , etc. If an inelastic collision of a photon having an initial energy $h\nu_0$ (h is the Plank constant, ν_0 is the electromagnetic frequency) with an unexcited molecule located at the lower energy level E_0 occurs, then the photon excites the molecule to a higher energy level E_1 . After such a collision, the photon scatters away from the molecule with reduced energy (here, the “ r ” index denotes the word “red”):

$$h\nu_r = h\nu_0 - (E_1 - E_0) . \quad (1.2)$$

If an inelastic collision of a photon with an already excited molecule occurs, then the molecule may undergo a transition from the level E_1 to the level E_0 , and the photon scatters with increased energy (the “ b ” index means “blue”):

$$h\nu_b = h\nu_0 + (E_1 - E_0). \quad (1.3)$$

In the first case, a quantum of intramolecular energy is subtracted from the initial energy of the light photon and, in the second case, the addition of this quantum occurs. In the first case, the frequency of the scattered photon appears to be less than the frequency of the photon incident on the molecule:

$$\nu_r = \nu_0 - \frac{E_1 - E_0}{h}, \quad (1.4)$$

and in the second, it is greater:

$$\nu_b = \nu_0 + \frac{E_1 - E_0}{h}. \quad (1.5)$$

Thus, together with the frequency ν_0 that exists as the result of the elastic collisions of photons with molecules, the frequencies ν_r and ν_b should appear in the scattered light. Correspondingly, in the spectrum of scattered light, two spectral lines (satellites) symmetrically shifted with respect to the centre line with a frequency ν_0 should be anticipated. The red satellite ν_r arises at longer wavelengths (this is why it is called “red”) as a result of the collisions of photons with molecules in a ground state, while the blue ν_b at shorter wavelengths (thus, “blue”) is due to collisions with excited molecules.

French physicists J. Cabannes, P. Daure and Y. Rocard were the first to try to experimentally confirm the predictions of the theorists, but they failed to measure the light of low intensity in gases.

The effect of inelastic scattering in liquids and vapours was first experimentally discovered by Chandrasekhara Venkata Raman and Kariamanickam Srinivasa Krishnan and reported in March of 1928 in “Nature” (Raman and Krishnan 1928). In this first work, Raman and Krishnan used a simple yet elegant experimental setup in which sunlight was focused by a telescope on scattering materials, thoroughly purified liquids or dust-free gases, and the method of complementary light filters was applied to visually observe “a modified scattered radiation”:

“A blue-violet filter, when coupled with a yellow-green filter and placed in the incident light, completely extinguished the track of the light through liquid or vapour. The reappearance of the track when the yellow filter is transferred to a place between it and the observer’s eye is proof of the existence of a modified scattered radiation” (Fig. 1-1).

Initially, Raman and Krishnan were looking for a new type of secondary radiation, as they assumed that there was an optical analogue to the Compton effect observed when X-rays are scattered by some materials. Nevertheless, they examined more than sixty common liquids and vapours and detected the modified scattered radiation with a changed frequency in each of the liquids to a greater or lesser degree.

In the same year, Russian physicists G.S. Landsberg and L.I. Mandelstam detected the phenomenon in crystals and published their work in a German-language journal “Die Naturwissenschaften” (“The Natural Sciences”) in July (Landsberg and Mandelstam 1928). They used a spectroscopic method of detection: an intense beam of light from a mercury lamp passed through a quartz crystal, and the light scattered off the crystal at 90° angle to the incident beam was investigated using a spectrograph. It was found that, in all spectrograms, each spectral line of mercury was accompanied by a

clearly observed satellite with a slightly longer wavelength. Soon after, Cabannes and Daure (Cabannes and Daure 1928) confirmed the discovery made by Raman and Krishnan, while Rocard published the first theoretical explanation of the phenomenon (Rocard 1928).

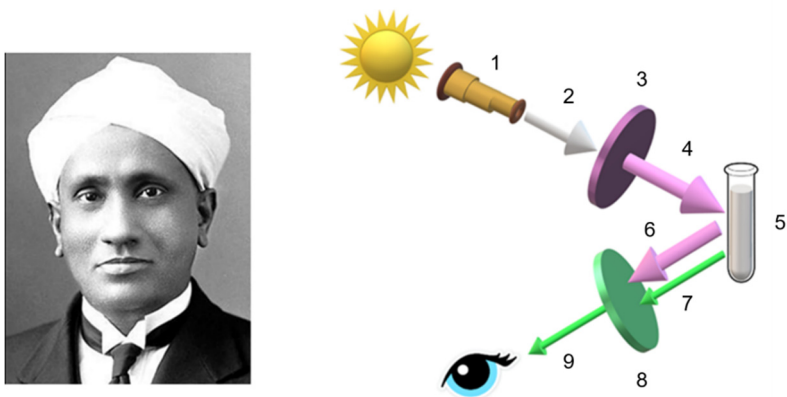


Figure 1-1. Sir Chandrasekhara Venkata Raman, the recipient of the Nobel Prize for Physics in 1930, and the schematic of his remarkable experiment described in “Nature”: 1 – telescope, 2 – incident sunlight (white) as the excitation light, 3 – blue-violet filter, 4 – blue-violet light transmitted through the filter, 5 – sample, 6 – unmodified (elastically) scattered light, 7 – modified (inelastically) scattered light, 8 – yellow-green filter, 9 – modified (inelastically) scattered yellow-green light passed through the filter to the observer’s eye.

It should be emphasized that all three groups of scientists from India, Russia and France, which investigated the phenomenon of molecular scattering of light, conducted their work entirely independently of each other.

Sir Chandrasekhara Venkata Raman was awarded the Nobel Prize for Physics in 1930 for his remarkable experimental discovery and proof of the universal character of this effect by investigating a large number of solids

and liquids, and the first publication of a spectrum of scattered light with changing frequencies. Raman scattering is named after him.

The intriguing history of this discovery, the Nobel Prize nomination and the award decision that underlined the importance of prompt research publications, relations and communications in the scientific community, with vast references to the original publications may be found elsewhere (Fabelinskii 1998, Singh and Reiss 2001, Singh 2018).

In 2028, the scientific community and the researchers dealing with molecular spectroscopy throughout the world will be celebrating the 100th anniversary of the outstanding discovery of the Raman effect. The author hopes that this book will still be available and useful at that time.

1.1.1. Fundamentals of Raman scattering

Historically, Raman scattering has been approached both in terms of classical electromagnetic and quantum-mechanical theories. In the classical approach, light is treated as an electromagnetic wave that propagates through and interacts with a matter. In turn, the matter is considered as consisting of atoms or molecules representing an assembly of independent harmonic oscillators. As is known, a molecule consists of positively charged nuclei surrounded by a negatively charged cloud of electrons. Although the total charge on a molecule is zero, positive and negative charges often do not entirely overlap. The molecules with these charges separated by small distances have a permanent dipole moment.

In this chapter, the GaussView 6 software package was used to visualise electrostatic potential maps of small molecules, such as diatomic O₂, triatomic CO₂ and H₂O. The full geometry optimization of the electrostatic

potential of the molecules with and without an external electric field, as well as the dipole moment and the polarizability changes during the molecular vibrations were performed using the Gaussian 16 computational chemistry software package (Gaussian n.d.). All calculations (Pushkarchuk 2019) were carried out using Density Functional Theory (DFT). Becke's three-parameter exchange functional in combination with the Lee-Yang-Parr correlation functional (B3LYP) and 6-31+G(3d) basis set were used (DFT/B3LYP/6-31+G(3d) level of the theory).

Consider a homonuclear diatomic molecule in an oscillating electric field, as shown in Figure 1-2.

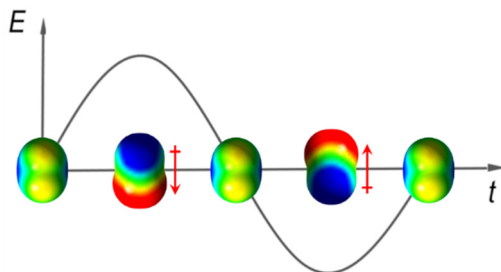


Figure 1-2. Interaction of the electric field E of the light wave with a homonuclear diatomic molecule. The perturbation of the electron cloud with time t results in a periodic separation of the centres of positive and negative charges within the molecule, which creates an induced dipole moment indicated by red vertical arrows.

The homonuclear diatomic molecule has no permanent dipole moment μ and, in the absence of an external electric field or when the amplitude of the electric field is equal to zero, the centre of the negative charge of the electron cloud coincides with the centre of the positively charged nuclei. The electric field of the light wave E oscillates with time t as a cosine function

$$E = E_0 \cos(2\pi \nu_0 t), \quad (1.6)$$

where E_0 is the magnitude of the electric field and ν_0 is the frequency of the light wave in Hz ($\nu = c/\lambda$, where c is the speed, and λ is the wavelength of light). The oscillating electric field perturbs the cloud of electrons surrounding the nuclei and displaces the centre of the electron cloud relative to the centre of the nuclei. The high and low electron density distribution is shown in red and blue, respectively. The displacement results in an induced dipole moment. In the literature, it is sometimes referred to as induced polarization and, to distinguish it from the permanent dipole moment usually indicated by μ , it is denoted as p :

$$p = \alpha E, \quad (1.7)$$

where α is the polarizability of the molecule. As follows from the equations (1.6) and (1.7), the oscillation of the induced dipole moment p occurs with the frequency ν_0 of the light wave:

$$p = \alpha E_0 \cos(2\pi \nu_0 t). \quad (1.8)$$

The polarizability α of the molecule is an important parameter in the classical theoretical consideration of the Raman effect. The polarizability can be described as a measure of deformability of the electron cloud in the molecule or, in other words, how easily the electron cloud can be distorted by the electric field of light interacting with the molecule. The polarizability α is not constant because the vibrations of atoms in the molecule can cause it to alter. During the vibration, the diatomic molecule is being consecutively compressed and extended. The configuration of the electron cloud is not the same at the two extremes of the vibration, so a change in polarizability occurs. However, the change happens at the frequency of

molecular vibrations ν_{vib} , which is much lower than the frequency of the light wave ν_0 . If the molecule is vibrating as a harmonic oscillator with a frequency ν_{vib} , then the displacement of nuclei q relative to an equilibrium position is given by the similar cosine function:

$$q = q_0 \cos(2\pi \nu_{vib} t), \quad (1.9)$$

where q_0 is the amplitude of vibration. For a diatomic molecule, such as O_2 , N_2 and H_2 , the displacement is about 10% of the distance between the nuclei at their equilibrium position. For such small displacements, the polarizability of the diatomic molecule can be described as a linear function of the displacement q . It can be expanded as a Taylor series around its equilibrium position $q = 0$ in which the higher-order terms can be neglected:

$$\alpha = \alpha_0 + \left(\frac{\partial\alpha}{\partial q}\right)_0 q + \dots, \quad (1.10)$$

where α_0 is the polarizability at the equilibrium position of the nuclei and the derivative $(\partial\alpha/\partial q)_0$ is the rate of change of the polarizability α upon the displacement of nuclei q from the equilibrium position $q=0$. Figure 1-3 illustrates the polarizability of a diatomic molecule during its vibration. For clarity, the displacement of nuclei from their equilibrium position defined by the bond length l in the compressed ($l-q_0$) and the extended ($l+q_0$) states is exaggerated. When the molecule is compressed, the electron cloud is imagined as mostly localized around the nuclei (the high and the low electron densities are close to each other) and therefore cannot be much distorted by an external electric field E . In contrast, when the molecule is expanded, the electron cloud appears to be delocalized (the high and the low electron densities are much further apart) and can thus be more readily

displaced by the electric field. Consequently, polarizability increases as the distance between the nuclei (bond length) elongates.

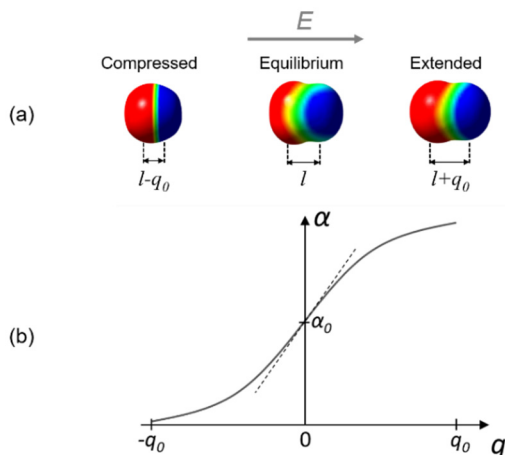


Figure 1-3. Polarizability of a diatomic molecule in an external electrical field E during its vibration. (a) The change of the electron density distribution: the high and the low electron density are shown in red and blue, respectively. (b) The graph representing the polarizability α as a function of displacement q (solid curve) and the derivative of polarizability $(\partial\alpha/\partial q)_0$ near the equilibrium position (dotted line).

Combining (1.8) through (1.10), and taking into account the known

trigonometric equation $\cos(2\pi\nu_0 t)\cos(2\pi\nu_{vib} t) = 1/2\cos[2\pi(\nu_0 + \nu_{vib})t] + 1/2\cos[2\pi(\nu_0 - \nu_{vib})t]$, the expression for the oscillating induced dipole moment takes the following form:

$$\begin{aligned}
 p &= \alpha E_0 \cos(2\pi\nu_0 t) = \alpha_0 E_0 \cos(2\pi\nu_0 t) + \\
 &\quad \left(\frac{\partial\alpha}{\partial q}\right)_0 q E_0 \cos(2\pi\nu_0 t) =
 \end{aligned}
 \tag{1.11}$$

$$\begin{aligned}
&= \alpha_0 E_0 \cos(2\pi \nu_0 t) + \\
&\left(\frac{\partial \alpha}{\partial q}\right)_0 q_0 E_0 \cos(2\pi \nu_0 t) \cos(2\pi \nu_{vib} t) = \\
&= \alpha_0 E_0 \cos(2\pi \nu_0 t) + \frac{1}{2} \left(\frac{\partial \alpha}{\partial q}\right)_0 q_0 E_0 \cos[2\pi (\nu_0 + \nu_{vib}) t] + \\
&\quad \frac{1}{2} \left(\frac{\partial \alpha}{\partial q}\right)_0 q_0 E_0 \cos[2\pi (\nu_0 - \nu_{vib}) t] .
\end{aligned}$$

The oscillating induced dipole moment represents a source that gives rise to scattered light. As follows from (1.11), there are three components in the scattered light. The first component has the same frequency ν_0 as the incident light and corresponds to Rayleigh scattering, which is the dominant effect. The two other components are shifted with respect to the frequency of the incident light by plus or minus the frequency of the molecular vibration and correspond to Raman scattering. The increase in frequency is referred to as an anti-Stokes (ν_{aS}) shift and the decrease in frequency is known as a Stokes (ν_S) shift:

$$\nu_{aS} = \nu_0 + \nu_{vib} , \quad \nu_S = \nu_0 - \nu_{vib} . \quad (1.12)$$

This terminology originates from the shift between the frequencies of the absorption and emission, which was observed by Irish physicist George Gabriel Stokes in the phenomenon of fluorescence in 1852 and named in his honour. According to Stokes' rule, the frequency of fluorescent light is always smaller or equal to that of the exciting light. Thus, the Stokes frequency corresponds to Stokes' rule, and the anti-Stokes frequency contradicts it. By analogy, this nomenclature was accepted for the Raman effect, although it differs from fluorescence.

The classical description correctly explains the frequencies of Rayleigh and Raman components in scattered light, provides a pictorial representation of the polarizability of molecules and predicts some other aspects of the scattering phenomenon. The energy emitted by an oscillating electric dipole per unit of time and integrated over a sphere enclosing the dipole is given by a known equation from the classical theory of radiation:

$$W = \frac{32\pi^4\nu_0^4}{3c^4} \alpha_0^2 E_0^2 \cos^2(2\pi\nu_0 t).$$

Averaging by time, the total energy elastically scattered by the induced dipole is as follows:

$$\bar{W}_R = \frac{16\pi^4\nu_0^4}{3c^4} \alpha_0^2 E_0^2,$$

since the average of cosine $\overline{\cos^2(2\pi\nu_0 t)} = 1/2$. Similarly, and taking into consideration factor $1/2$ for the terms of Raman scattering in (1.11), the total time-averaged energies inelastically scattered with Stokes and ant-Stokes shifts can be presented, correspondingly, as

$$\bar{W}_S = \frac{4\pi^4(\nu_0 - \nu_{vib})^4}{3c^4} \left(\frac{\partial\alpha}{\partial q}\right)^2 q_0^2 E_0^2 \quad (1.13)$$

and

$$\bar{W}_{as} = \frac{4\pi^4(\nu_0 + \nu_{vib})^4}{3c^4} \left(\frac{\partial\alpha}{\partial q}\right)^2 q_0^2 E_0^2. \quad (1.14)$$

Thus, the total energy of light scattered by a single molecule is proportional to the fourth power of the frequency, the square of the amplitude of the electric field E_0 of the incident light and the square of the polarizability of the molecule. Since, if plotted in the coordinate axes of Figure 1-3, $(\partial\alpha/\partial q)_0$

appears to be much smaller than α_0 , then Raman scattering is also predicted to be much weaker than Rayleigh scattering.

However, one of the major limitations of the classical theory is the inference that the energies of Stokes and corresponding anti-Stokes Raman components should be approximately the same. Indeed, dividing the expression (1.13) by (1.14) the ratio results in

$$\frac{\bar{W}_S}{\bar{W}_{aS}} = \frac{(\nu_0 - \nu_{vib})^4}{(\nu_0 + \nu_{vib})^4} \approx 1.$$

Another limitation of the classical theory is that it does not take the real physical states of the molecules involved in the interaction with the incident light into consideration. The basic concepts of the classical consideration of Rayleigh and Raman scattering are illustrated in Figure 1-4.

This and other limitations of the classical approach can be overcome exclusively in frames of the quantum-mechanical theory that reveals the reality of physics on a molecular scale by introducing the quantized energy states of both the radiation and molecules. The quantum theory considers radiation and the molecule together as a complete system and describes how energy is transferred between the radiation and the molecule as a result of the interaction. The molecule is described by the Schrödinger equation, which takes the movement of electrons, the vibrations of atoms relative to each other in a molecule and the rotation of the molecule as a whole into account. A detailed quantum-mechanical description of the Raman effect is rather complicated and beyond the scope of this book. Although there are many detailed texts on the quantum-mechanical interpretation of Raman scattering, the reader is referred to the book by Long (Long 2002), which

presents a unified theoretical approach in a complete and comprehensible form.

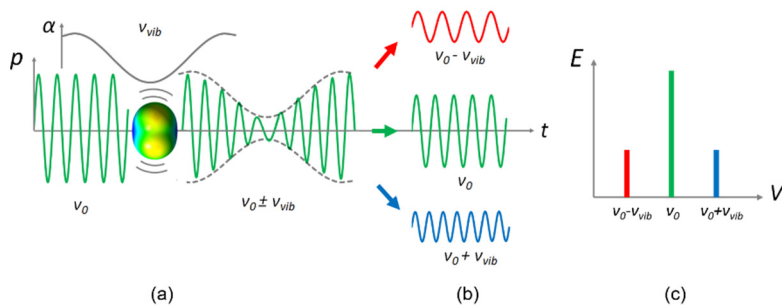


Figure 1-4. Schematic representation of basic concepts of the classical theory of Rayleigh and Raman scattering. (a) The incident light induces the dipole moment p in the molecule and makes it oscillate at the frequency ν_0 of the incident light. The vibration of nuclei at a much lower frequency ν_{vib} changes the polarizability α of the molecule. As a result, the amplitude of the lightwave reemitted by the induced dipole moment is modulated. (b) The amplitude-modulated wave has three components: the carrier wave of the frequency ν_0 (Rayleigh scattering), two sidebands with the frequencies $\nu_0 - \nu_{vib}$ (Stokes Raman scattering) and $\nu_0 + \nu_{vib}$ (anti-Stokes Raman scattering), which are shown as cosine waves in the time domain t . (c) The same components of scattered light in the frequency domain ν are denoted by the colours corresponding to the Stokes (red) and anti-Stokes (blue) Raman shifts with respect to the Rayleigh component (green) of unchanged frequency. Note, the amplitudes of the Stokes and anti-Stokes Raman components are equal.

According to quantum mechanics, an isolated molecule can only exist in quantized energy states that, in the general case, can be represented by electronic, vibrational and rotational levels of energy. The quantized energy levels of molecules and transitions between them when interacting with photons of light can be graphically represented in the form of a Jablonski

diagram. In the diagram introduced by and named after the Polish physicist Aleksander Jablonski, the states are arranged vertically by energy and grouped horizontally by corresponding transitions. As mentioned earlier, in the quantum-mechanical interpretation proposed by Kramers, Heisenberg and Dirac, the Raman effect is described as an inelastic scattering of a photon by a vibrating molecule. Figure 1-5 illustrates the process formulated in the sequence of simple equations (1.2)–(1.5) above and determines some additional information.

For the sake of simplicity, consider a ground electronic state E_0 with only two corresponding vibrational levels of energy denoted by quantum numbers 0 and 1 for the ground and excited level, respectively. The rotational energy levels are ignored since their energy is significantly lower than the energy of vibrations, and the rotation motion is hindered in a condensed matter. The incident photon excites the molecule from an initial energy state to a virtual E_{virt} state, as shown in Figure 1-5(b). A virtual state is a very short-lived intermediate quantum state that is not defined by a strict molecular energy value. From the virtual state, the molecule instantaneously relaxes back to a vibrational level in the ground E_0 electronic state and emits a photon of light. When the relaxation occurs, there are three possible situations. First, the molecule is excited from and then relaxes down to the same ground vibrational level 0 and reemits a photon of light with the energy equal to that of the incident photon. As we know, this is an elastic process that corresponds to Rayleigh scattering with the unchanged frequency of the light. The other two situations result in the inelastic scattering of the incident photon that alters its energy. If the molecule is excited by a photon from